Inorganic Chemistry

Article

pubs.acs.org/IC

Selective Sensitization of Eu(III) and Tb(III) Emission with Triarylboron-Functionalized Dipicolinic Acids

Hee-Jun Park, Soo-Byung Ko, Ian W. Wyman, and Suning Wang*

Department of Chemistry, Queen's University, Kingston, Ontario K7L 3N6, Canada

Supporting Information

ABSTRACT: Three triarylboron- (Mes_2BAr-) functionalized dipicolinic acids, namely, 4-(4-(dimesitylboranyl)-2,3,5,6-tetramethylphenyl)pyridine-2,6-dicarboxylic acid (H_2**L1**), 4-(4-(4-dimesitylboranyl)-2,3,5,6-tetramethylphenyl)-1*H*-1,2,3-triazol-1-yl)pyridine-2,6-dicarboxylic acid (H_2**L2**), and 4-(4-(4-dimesitylboranyl) phenyl)-1*H*-1,2,3-triazol-1-yl)pyridine-2,6-dicarboxylic acid (H_2**L3**), have been designed and synthesized. Lanthanide(III) complexes with the general formula of $[NBu_4]_3[LnL_3]$ (Ln = Eu or Tb; L = **L1**, **L2**, or **L3**) were obtained. The new triarylboron-functionalized ligands were found to be effective in the selective sensitization of the emissions of Eu(III) and Tb(III) ions with a high quantum efficiency (e.g., 0.54 for $[NBu_4]_3[Tb$**L1**$_3]$ in the solid state) upon excitation at ∼330 nm. An intraligand charge-transfer (ILCT) transition from the mesityl or aryl group to the boron or boron-aryl unit was found to play a key role in the activation of the Eu(III) and Tb(III) emissions, based on TD-DFT computational data and luminescence titration experiments performed using fluoride and cyanide ions.

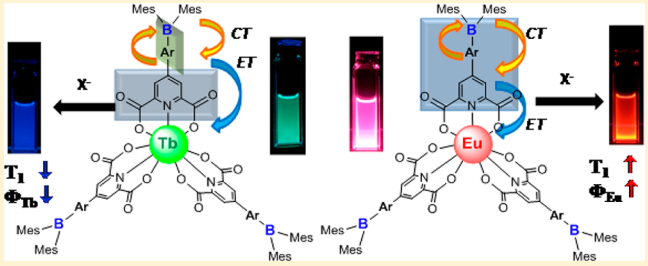

INTRODUCTION

Trivalent lanthanide ions Ln(III), such as Eu(III) and Tb(III), exhibit distinct and well-defined narrow emission bands from f−f transitions that have long decay lifetimes and large Stokes shifts, enabling the use of lanthanide compounds in organic light-emitting devices (OLEDs),[1] bioimaging,[2] sensing,[3] and time-resolved luminescent immunoassays.[4] Lanthanide metal complexes have also been used effectively in anion sensing.[5,6] Because of their symmetry-forbidden f−f transitions, Ln(III) ions usually have a very small molar extinction coefficient ($<10^{-1}$ M^{-1} cm^{-1}) and very weak emission intensity.[7] This problem can be overcome, however, through the introduction of an appropriate antenna ligand that can activate the lanthanide emission through indirect excitation or energy transfer.[2−6,8] Ideal antenna ligands must be able to harvest light efficiently and have a suitable T_1 energy for efficient energy transfer to the emissive state of the Ln(III) ion, in addition to being an effective chelate ligand to saturate the coordination sphere of the Ln(III) ion. Many antenna ligands have been developed for lanthanide complexes.[9−12]

An important class of ligands for lanthanide complexes is dpa (pyridine-2,6-dicarboxylate or dipicolinate) and its derivatives,[10c−e,13,14] which form coordinatively saturated and very stable[13a] nine-coordinated Ln(III) complexes and capable of activating Tb(III) or Eu(III) emission.[10c−e,14] The dpa molecule is a convenient biomarker for the anthrax spore,[15] and because of its strong binding to lanthanide ions, many anthrax sensors are based on lanthanide compounds.[16] Hence, to achieve robust, highly emissive, and functional lanthanide compounds, dpa-based systems are very attractive. However, one key problem with Ln-dpa complexes is the requirement of excitation at $\lambda \leq 300$ nm, which seriously limits the use of this class of compounds in biosensing and materials applications. One way to overcome this problem is to introduce functional groups onto the dpa ligand such that the excitation energy can be shifted to the 300−400-nm region. Functionalizing dpa is difficult, however, because of the presence of multiple reactive sites. In fact, only a few examples of functionalized dpa ligands are known.[10c−e,14] Recently, it was shown that the introduction of an intraligand charge-transfer (ILCT) state on the dpa ligand can be highly effective in red shifting the excitation energy and sensitizing Eu(III) emission.[10c,e,14]

One functional group that might be effective in red shifting the excitation energy of dpa is $BMes_2Ar$ (Mes = mesityl). Compounds with this unit are known to display a distinct low-energy ILCT transition (Mes/Ar to B or a donor group on Ar to B)[6,17,18] and are highly selective sensors for small anions such as F^- and CN^-.[17,18] We recently showed that $BMes_2Ar$-functionalized carboxylates (p-$BMes_2ArCO_2^-$)[6a] and β-diketonato ligands[6b] could be very effective in sensitizing the luminescence of Tb^{3+} or Eu^{3+} ions, depending on the linker unit and the position of the boryl unit, and that the resulting complexes could be used as visual indicators/sensors for fluoride or cyanide.[6] However, because monocarboxylate ligands cannot saturate the coordination sphere of the lanthanide ion, their complexes form oligomeric species with a poor solubility in common organic solvents. Furthermore, the

Received: June 7, 2014
Published: August 22, 2014

   dx.doi.org/10.1021/ic501335e | *Inorg. Chem.* 2014, 53, 9751−9760

Scheme 1. (Top) Concept of Using Switchable ILCT to Sensitize Ln(III) Emission. (Bottom) Structures of the New $BMes_2Ar$-Functionalized dpa Ligands

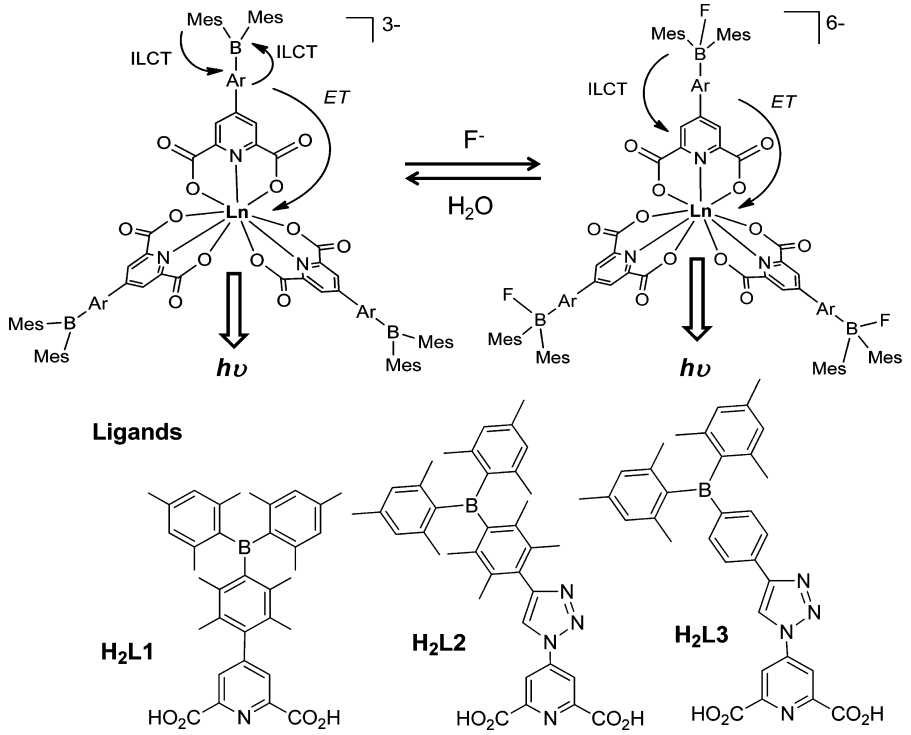

monocarboxylate Ln(III) compounds are prone to coordination by other donor ligands such as H_2O and OH^- in solution, thus complicating their use as luminescent dyes/probes. Similar problems were also observed with lanthanide compounds based on $BMes_2$-functionalized β-diketonato ligands,[6b] albeit to a lesser degree. These shortcomings of p-$BMes_2ArCO_2^-$ ligands or $BMes_2$-functionalized β-diketonato ligands could be addressed if the monocarboxylate or β-diketonato unit were replaced by a dicarboxylate unit such as dpa that can bind to the Ln^{3+} ion as a tridentate chelate ligand. A key advantage of incorporating a $BMes_2Ar$ unit in dpa is the possibility of switching the energy of the ILCT state by adding anions such as fluoride ions, which could provide further control/tuning of the emission efficiency of the Ln(III) compounds, as shown in Scheme 1. Based on these considerations, we designed and synthesized the three $BMes_2Ar$-functionalized dpa ligands shown in Scheme 1. These new ligands combine the strong chelating ability of the dpa unit with the ILCT state and anion-sensing/-binding ability of the $BMes_2Ar$ group. Highly emissive and stable Tb(III) and Eu(III) compounds based on the new ligands were achieved. The details of the new ligands and their Ln^{3+} complexes and the use of the complexes in anion sensing are reported herein.

EXPERIMENTAL SECTION

The syntheses of all ligands were carried out under a nitrogen atmosphere using standard Schlenk line techniques. Tetrahydrofuran (THF) was dried over Na/benzophenone and was subsequently distilled under nitrogen prior to use. The syntheses of the starting materials (p-iododuryl)dimesitylborane (**A**),[18c] dimethyl-4-(pinacolatoboronic ester)-2,6-dicarboxylate (**B**),[14c] dimethyl 4-azidopyridine-2,6-dicarboxylate (**C**),[10c] (p-ethynylduryl)dimesitylborane (**D**),[18c] and p-$BMes_2$-phenylacetylene (**E**)[19] were accomplished according to previously reported methods. Deuterated solvents $CDCl_3$ and dimethyl sulfoxide (DMSO) were purchased from Cambridge Isotopes and used as obtained without additional purification. ^1H, ^{13}C, and ^{19}F NMR spectra were recorded on a Bruker 500 spectrometer. UV−vis absorption spectra were recorded on a Varian Cary 50 spectrometer. Phosphorescence spectra and decay lifetimes were recorded using a PTI Time Master Pro spectrometer. Total emission spectra were recorded on a Photon Technologies International QuantaMaster 2 spectrometer. Solid-state emission data were recorded using a PTI integration sphere simultaneously with the fluorimeter. Elemental analyses were performed at the Elemental Analysis Laboratory at the University of Montreal, Montreal, Quebec, Canada. High-resolution mass spectrometry (HRMS) data were recorded on a Micromass/Waters GCT time-of-flight (TOF) mass spectrometer and a Thermo Scientific Orbitrap Velos Pro mass spectrometer. The computational work was performed using the Gaussian 09[20] software package and the High Performance Computing Virtual Laboratory (HPCVL) at Queen's University (Kingston, Ontario, Canada). The ground-state geometries were fully optimized with the CAM-B3LYP[21] exchange-correlation functional using the 6-31G(d) basis set.[22] The initial geometric parameters of H_2**L3** were based on the crystal structural parameters of **3** and used for geometry optimizations. Time-dependent density function theory (TD-DFT) calculations were performed to obtain the vertical singlet and triplet excitation energies.

Synthesis of Ester 1. (p-Iododuryl)dimesitylborane (**A**, 508 mg, 1.0 mmol, 1.0 equiv), dimethyl-4-(pinacolatoboronic ester)-2,6-dicarboxylate (**B**, 353 mg, 1.1 mmol, 1.1 equiv), $Pd_2(dba)_3$ (46 mg, 0.05 mmol, 0.05 equiv), and $[HP(t\text{-}Bu)_3]BF_4$ (29 mg, 0.1 mmol, 0.10 equiv) were mixed in 6 mL of THF at room temperature. An aqueous solution of Na_2CO_3 (530 mg, 5.0 mmol, 5.0 equiv) was then added to the solution. After being stirred for 9 h at room temperature, the reaction mixture was extracted with dichloromethane, washed with water, and dried with $MgSO_4$. The product **1** was purified by column chromatography using ethyl acetate/hexane (1:3) as the eluent. Yield: 150 mg (26%). ^1H NMR (500 MHz, $CDCl_3$, ppm): δ = 8.10 (s, 2H), 6.74 (s, 4H), 4.02 (s, 6H), 2.25 (s, 6H), 2.00 (s, 6H), 1.99 (s, 6H), 1.96 (s, 6H), 1.76 (s, 6H). ^{13}C NMR (125 MHz, $CDCl_3$, ppm): δ = 165.36, 154.71, 148.40, 144.32, 140.93, 140.68, 139.47, 138.32, 135.76, 130.05, 129.42, 128.92, 128.81, 53.25, 23.24, 22.83, 21.24, 20.15, 17.71. HRMS: calcd for $C_{37}H_{42}N_1O_4B_1$, 575.3207; found, 575.3226.

dx.doi.org/10.1021/ic501335e | Inorg. Chem. 2014, 53, 9751−9760

Scheme 2. Synthetic Procedures for the New Ligands and the Ln(III) Complexes

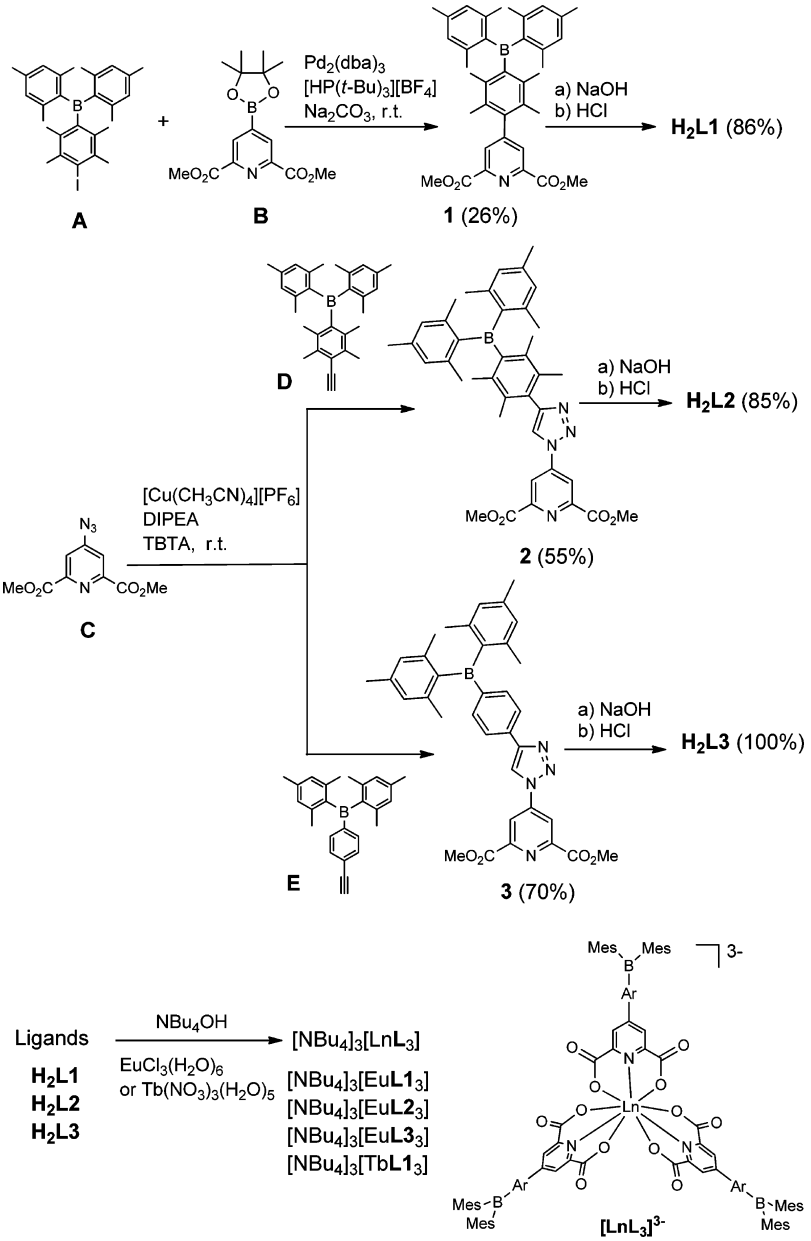

Synthesis of Ester 2. 4-Azidopyridine-2,6-dicarboxylate (**C**, 182 mg, 0.77 mmol, 1.0 equiv) and (*p*-ethynylduryl)dimesitylborane (**D**, 345 mg, 0.85 mmol, 1.1 equiv) were dissolved in 15 mL of CH_2Cl_2. Diisopropylethylamine (DIPEA, 0.27 mL, 2.0 equiv), tris[(1-benzyl-1*H*-1,2,3-triazol-4-yl)methyl]amine (TBTA, 4 mg, 0.008 mmol, 0.01 equiv), and $[Cu(CH_3CN)_4][PF_6]$ (3 mg, 0.008 mmol, 0.01 equiv) were added to the solution. After being stirred for 10 h at room temperature, the reaction mixture was washed with NH_4Cl (aq) and water and dried with $MgSO_4$. The product **2** was purified by column chromatography using ethyl acetate as the eluent. Yield: 272 mg (55%). ^{1}H NMR (500 MHz, $CDCl_3$, ppm): δ = 8.80 (s, 2H), 8.20 (s, 1H), 6.72 (s, 4H), 4.03 (s, 6H), 2.24 (s, 6H), 2.01 (s, 6H), 1.99 (s, 6H), 1.95 (s, 6H), 1.91 (s, 6H). ^{13}C NMR (125 MHz, $CDCl_3$, ppm): δ = 164.21, 150.48, 149.82, 149.54, 145.44, 144.35, 140.92, 140.74, 139.42, 135.55, 133.16, 129.31, 128.88, 128.80, 120.27, 117.42, 53.58, 23.24, 22.91, 21.25, 20.26, 17.63. HRMS: calcd for $C_{39}H_{43}N_4O_4B_1$, 642.3377; found, 642.3405.

Synthesis of Ester 3. 4-Azidopyridine-2,6-dicarboxylate (**C**, 202 mg, 0.86 mmol, 1.0 equiv) and *p*-(dimesitylboryl)phenylacetylene (**E**, 330 mg, 0.94 mmol, 1.1 equiv) were dissolved in 15 mL of CH_2Cl_2. DIPEA (0.3 mL, 2.0 equiv), TBTA (5 mg, 0.009 mmol, 0.01 equiv), and $[Cu(CH_3CN)_4][PF_6]$ (3.2 mg, 0.009 mmol, 0.01 equiv) were added to the solution. After being stirred for 10 h at room temperature, the reaction mixture was washed with NH_4Cl (aq) and water and dried with $MgSO_4$. The product **3** was purified by column chromatography using ethyl acetate as the eluent. Yield: 353 mg (70%). ^{1}H NMR (500 MHz, $CDCl_3$, ppm): δ = 8.77 (s, 2H), 8.53 (s, 1H), 7.90 (d, J = 8.0 Hz, 2H), 7.62 (d, J = 8.0 Hz, 2H), 6.82 (s, 4H), 4.06 (s, 6H), 2.30 (s, 6H), 2.01 (s, 12H). ^{13}C NMR (125 MHz, $CDCl_3$, ppm): δ = 164.19, 150.52, 149.47, 146.83, 145.20, 141.55, 140.86, 138.91, 137.04, 132.06, 128.28, 125.52, 117.46, 117.43, 53.65, 23.48, 21.25. HRMS: calcd for $C_{35}H_{35}N_4O_4B_1$: 586.2751; found, 586.2771.

Synthesis of H_2L1. To 7.5 mL of mixed solvent (THF/water, 1:2) were added ester **1** (150 mg, 0.26 mmol, 1.0 equiv) and 1.6 mL (6.0 equiv) of aqueous NaOH (1 M). The reaction mixture was stirred at 50 °C for 2 h. After the mixture had cooled to room temperature, HCl (2 M) was added dropwise until pH 5. The white precipitates were filtered and dried under a vacuum. Yield: 122 mg (86%). ^{1}H NMR (500 MHz, DMSO, ppm): δ = 7.89 (s, 2H), 6.79 (s, 4H), 2.23 (s, 6H),

dx.doi.org/10.1021/ic501335e | *Inorg. Chem.* 2014, 53, 9751−9760

1.98 (s, 12H), 1.92 (s, 6H), 1.76 (s, 6H). The ^{13}C NMR spectrum was not recorded because of the poor solubility of this compound. HRMS: calcd for $C_{35}H_{38}N_1O_4B_1$, 547.2894; found, 546.2832 ($M - H^+$).

Synthesis of H_2L2. The synthesis of this compound was accomplished using the same procedure as described for H_2**L1** but with ester **1** replaced by ester **2** (184 mg, 0.29 mmol, 1.0 equiv). Yield: 151 mg (85%). ^{1}H NMR (500 MHz, DMSO, ppm): δ = 9.26 (s, 1H), 8.66 (s, 2H), 6.79 (s, 4H), 2.24 (s, 6H), 2.00 (s, 12H), 1.93 (s, 6H), 1.91 (s, 6H). The ^{13}C NMR spectrum was not recorded because of the poor solubility of this compound. HRMS: calcd for $C_{37}H_{38}N_4O_4B_1$, 613.2986 ($M - H^+$); found, 613.2997.

Synthesis of H_2L3. The synthesis of this compound followed the same procedure as described for H_2**L1** but with ester **1** replaced by ester **3** (271 mg, 0.46 mmol, 1.0 equiv). Yield: 257 mg (~100%). ^{1}H NMR (500 MHz, DMSO, ppm): δ = 9.87 (s, 1H), 8.69 (s, 2H), 8.04 (d, J = 7.5 Hz, 2H), 7.50 (d, J = 8.0 Hz, 2H), 6.85 (s, 4 H), 2.28 (s, 6H), 1.97 (s, 12H). The ^{13}C NMR spectrum was not recorded because of the poor solubility of this compound. HRMS: calcd for $C_{33}H_{30}N_4O_4B_1$, 557.2360 ($M - H^+$); found, 557.2371.

Synthesis of Ln(III) Complexes. All Ln(III) compounds were synthesized using the general procedure described below.

To a suspension of an appropriate ligand (H_2**L1**, H_2**L2**, or H_2**L3**) in 20 mL of water was added [NBu_4][OH] (1.0 M in methanol). After the mixture had been stirred for 20 min, $EuCl_3{\cdot}6H_2O$ or $Tb(NO_3)_3{\cdot}5H_2O$ was added, and the resulting mixture was stirred for 2 h at room temperature. The reaction mixture was then extracted several times with CH_2Cl_2 (5 × 100 mL). The combined organic phases were concentrated to ~50 mL, washed several times with water (5 × 50 mL) to remove impurities, and concentrated in vacuo. The pure compounds were isolated as white solids by the slow evaporation of the solution of the Ln(III) compound in THF and water. Efforts to obtain single crystals suitable for X-ray diffraction analysis were unsuccessful. ^{1}H NMR spectra of the three Eu(III) complexes in $CDCl_3$ displayed broad but well-resolved peaks, whereas the ^{1}H NMR spectrum of **Tb-1** was only partially resolved (see SI).

*[NBu_4]$_3$[Eu**L1**$_3$] (**Eu-1**).* H_2**L1** (107 mg, 0.20 mmol, 3.0 equiv), $EuCl_3{\cdot}6H_2O$ (25 mg, 0.07 mmol, 1.05 equiv), and NBu_4OH, (1.0 M in methanol, 0.39 mL, 6.0 equiv) were reacted in the manner described above to produce **Eu-1**. Yield: 120 mg (70%). ^{1}H NMR (500 MHz, $CDCl_3$, ppm): δ = 6.65 (br, s, 12 H), 5.88 (br, s, 24 H), 4.91 (br, s, 6 H), 2.87 (br, s, 24 H), 2.21 (br, s, 24 H), 1.85 (br, s, 54 H), 1.70 (m, 36 H), 1.02 (br, s, 36 H). HRMS: calcd for $C_{121}H_{144}N_4O_{12}B_3Eu_1$ ($M - 2NBu_4^+$), 2031.0282; found, 2031.0322. Anal. Calcd for $C_{153}H_{216}N_6B_3O_{12}Eu_1{\cdot}10H_2O$, C 68.11, H 8.82, N 3.12; found, C 67.89, H 8.21, N 2.94.

*[NBu_4]$_3$[Eu**L2**$_3$] (**Eu-2**).* H_2**L2** (185 mg, 0.3 mmol, 3.0 equiv), $EuCl_3{\cdot}6H_2O$ (37 mg, 0.1 mmol, 1.05 equiv), and NBu_4OH (1.0 M in methanol, 0.6 mL, 6.0 equiv) were reacted in the same manner as described above to produce **Eu-2**. Yield: 52 mg (52%). ^{1}H NMR (400 MHz, $CDCl_3$, ppm): δ = 7.09 (br, s, 3H), 6.72 (s, 12H), 5.74 (br, s, 6H), 5.30 (br, s, 24H), 2.80 (br, s, 24H), 2.25 (s, 18H), 1.92 (br, s, 60H), 1.62 (s, 18H), 1.29 (s, 18H), 1.12 (br, s, 36H). HRMS: calcd for $C_{127}H_{147}N_{13}O_{12}B_3Eu_1$ ($M - 2NBu_4^+$), 2232.0784; found, 2232.0794. Anal. Calcd for $C_{159}H_{219}N_{15}B_3O_{12}Eu_1{\cdot}13H_2O$, C 64.71, H 8.37, N 7.12; found, C 64.35, H 8.11, N 6.94.

*[NBu_4]$_3$[Eu**L3**$_3$] (**Eu-3**).* H_2**L3** (115 mg, 0.21 mmol, 3.0 equiv), $EuCl_3{\cdot}6H_2O$ (26 mg, 0.07 mmol, 1.0 equiv), and [NBu_4][OH] (1.0 M in methanol, 0.42 mL, 6.0 equiv) were reacted in the same manner as described above to produce **Eu-3**. Yield: 89 mg (50%). ^{1}H NMR (500 MHz, $CDCl_3$, ppm): δ = 7.56 (d, J = 7.5 Hz, 6H), 7.53 (s, 3H), 7.46 (d, J = 7.5 Hz, 6H), 6.79 (s, 12H), 5.74 (s, 6H), 5.65 (br, s, 24H), 2.99 (br, s, 24H), 2.29 (s, 18H), 2.07 (br, s, 24H), 1.95 (br, s, 36H), 1.14 (br, s, 36H). HRMS: calcd for $C_{115}H_{123}N_{13}O_{12}B_3Eu_1$ ($M - 2NBu_4^+$), 2063.8905; found, 2063.8936. Anal. Calcd for $C_{147}H_{195}N_{15}B_3O_{12}Eu_1{\cdot}5H_2O$, C 66.86, H 7.83, N 7.96; found, C 66.89, H 7.67, N 7.36.

*[NBu_4]$_3$[Tb**L1**$_3$] (**Tb-1**).* H_2**L1** (211 mg, 0.39 mmol, 3.0 equiv), $Tb(NO_3)_3{\cdot}5H_2O$ (59 mg, 0.14 mmol, 1.05 equiv), and [NBu_4][OH] (1.0 M in methanol, 0.77 mL, 6.0 equiv) were reacted in the same manner as described above to produce **Tb-1**. Yield: 245 mg (72%). HRMS: calcd for $C_{121}H_{144}N_4O_{12}B_3Tb_1$ ($M - 2NBu_4^+$), 2037.0324; found, 2037.0400. Anal. Calcd for $C_{153}H_{216}N_6B_3O_{12}Tb_1{\cdot}8H_2O$, C 68.88, H 8.77, N 3.15; found, C 68.93, H 8.42, N 3.06.

X-ray Crystallographic Analysis. Single crystals of esters of **2** and **3** were obtained from CH_2Cl_2 solution by slow evaporation of the solvent at room temperature and mounted on glass fibers for data collection. Diffraction data were collected on a Bruker Apex II single-crystal X-ray diffractometer using graphite-monochromated Mo Kα radiation, operating at 50 kV and 30 mA and at 180 K. The structure was solved by direct methods (SHELXTL, version 6.14) and refined against all F^2 data. All non-hydrogen atoms were refined anisotropically. Complete crystal structure data were deposited at the Cambridge Crystallographic Data Center (CCDC 1005954 and 988595 for **2** and **3**, respectively).

RESULTS AND DISCUSSION

Synthesis and Crystal Structure. The three new dipicolinic acids H_2**L1**, H_2**L2**, and H_2**L3** were prepared using the procedures shown in Scheme 2. The ester compound **1** was synthesized by a Suzuki cross-coupling reaction between (iododuryl)dimesitylborane (**A**)[18c] and dimethyl-4-(pinacolato-boronic ester)-2,6-dicarboxylate (**B**)[14a] in 26% yield using $Pd_2(dba)_3$/[$HP(t\text{-}Bu)_3$][BF_4] as the catalyst and Na_2CO_3 as the base. A subsequent saponification of **1** with NaOH in a water/THF mixture produced H_2**L1** in 86% yield. For the synthesis of H_2**L2** and H_2**L3**, we employed a "click" reaction to introduce a triazole unit between the $BMes_2Ar$ unit and the dpa unit. The copper-catalyzed click reaction between dimethyl 4-azidopyridine-2,6-dicarboxylate (**C**)[24] and *p*-$BMes_2$-durylacetylene (**D**)[18c] produced **2** in 55% yield, whereas the reaction between **C** and *p*-$BMes_2$-phenylacetylene (**E**)[19] produced **3** in 70% yield. The subsequent saponification of **2** and **3** provided the desired ligands H_2**L2** and H_2**L3**, respectively, quantitatively. The structures of esters **2** and **3** were determined by X-ray diffraction analysis, and the crystal data are provided in the Supporting Information (SI). As shown in Figure 1, the phenyl linker is coplanar with the triazolyl ring and the dpa unit in **3**. In contrast, the duryl linker in **2** is perpendicular to the triazolyl ring and the dpa unit (dihedral angle ≈ 84°), whereas the triazolyl-dpa portion is coplanar. For comparison, the structures of all three ligands were calculated and optimized by DFT computational methods, as shown in Figure 2. In H_2**L1** and H_2**L2**, the dpa and triazolyl-dpa units are perpendicular to the duryl group, whereas in H_2**L3**, the triazolyl-dpa unit is coplanar with the phenyl linker.

The abilities of the new ligands to sensitize Eu(III) and Tb(III) emissions were first investigated by examining the luminescence characteristics of mixtures of the ligands with Eu(III) or Tb(III) ions [as $LnCl_3$, $Ln(NO_3)_3$, or Ln-(benzoate)$_3$]. Preliminary titration tests of $Tb(Bz)_3$ or $Eu(Bz)_3$ with H_2**L1**−H_2**L3** indicated that all three ligands are capable of sensitizing Eu(III) emission but only ligand H_2**L1** is capable of sensitizing the emission of Tb(III) (see SI). We therefore focused our synthetic efforts on four Ln(III) complexes only, namely, [NBu_4]$_3$[Eu**L1**$_3$] (**Eu-1**), [NBu_4]$_3$[Eu**L2**$_3$] (**Eu-2**), [NBu_4]$_3$[Eu**L3**$_3$] (**Eu-3**), and [NBu_4]$_3$[Tb**L1**$_3$] (**Tb-1**), which were prepared by the reaction of NBu_4OH with the appropriate ligand in a 2:1 ratio in THF and water, followed by the addition of either $EuCl_3{\cdot}6H_2O$ or $Tb(NO_3)_3{\cdot}5H_2O$ (Ln/ligand ratio =1:3), as shown in Scheme 2. The Ln(III) complexes were isolated in 50−70% yields. Efforts to grow single crystals of the Ln(III) compounds were unsuccessful.

Sensitization of Eu(III) and Tb(III) Emission. The absorption spectra of the lanthanide complexes are shown in Figure 3. The absorption/excitation spectra of the complexes

dx.doi.org/10.1021/ic501335e | Inorg. Chem. 2014, 53, 9751−9760

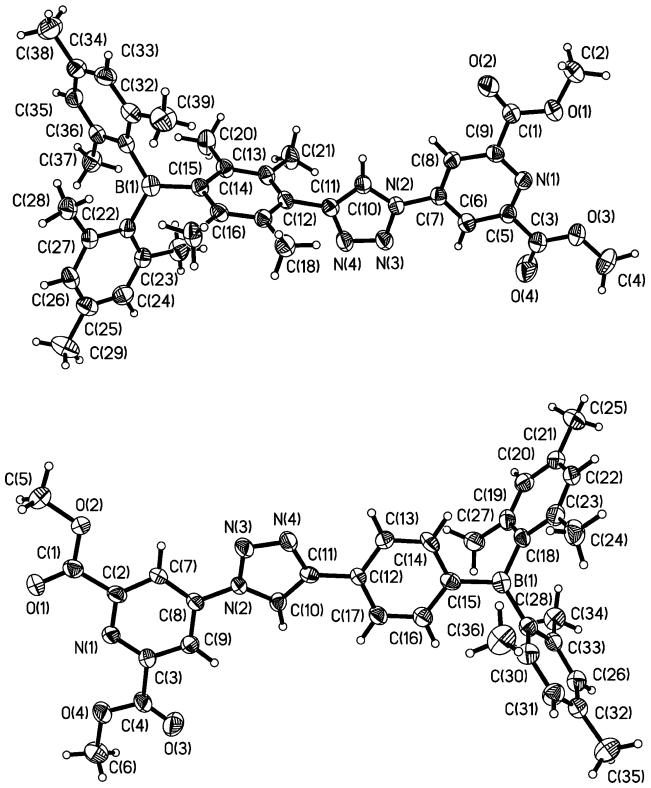

Figure 1. Crystal structures of **2** (top) and **3** (bottom) with 50% thermal ellipsoids and labeling schemes.

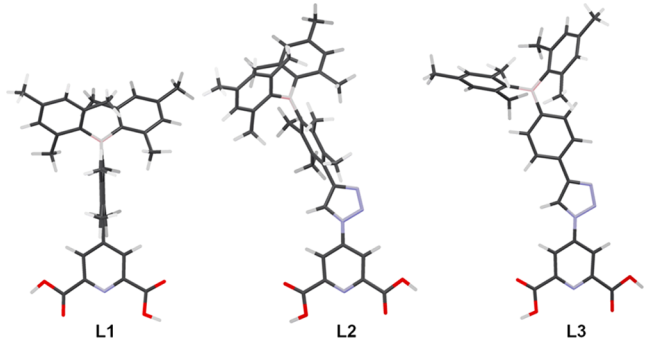

Figure 2. DFT-optimized structures of the $BMes_2Ar$-functionalized dpa ligands.

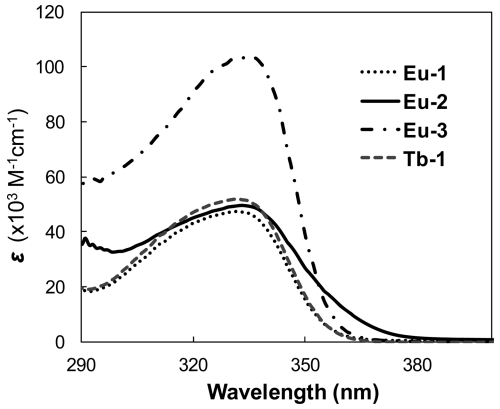

Figure 3. Absorption spectra of the Ln(III) complexes in THF.

closely resemble those of the corresponding free ligands (see SI) with λ_{max} at ~330 nm. Compared to the nonfunctionalized $[Ln(dpa)_3]^{3-}$ compounds,[13] the absorption bands of **Eu-1**, **Eu-2**, **Eu-3**, and **Tb-1** are red-shifted by more than 30 nm. Furthermore, the new ligands have very high extinction coefficients (see SI), which provide the lanthanide complexes intense absorption bands with $\lambda_{max} \approx 330$ nm (Table 1).

Table 1. Photophysical Properties of the Eu(III) and Tb(III) Complexes

compound	λ_{abs}[a] (nm) (ε, M^{-1} cm^{-1})	λ_{ex} (nm)	λ_{em}[a] (nm)	τ[b] (ms)	Φ_{ss} total/Ln(III) emission[c]
Eu-1	332 (47 400)	336	391, 594, 615, 695	1.87	0.37/0.30
Eu-2	333 (48 100)	341	395, 594, 615, 695	1.90	0.23/0.07
Eu-3	334 (104 000)	341	394, 594, 615, 695	1.67	0.26/0.17
Tb-1	332 (52 100)	336	387, 492, 545, 584, 622	0.80	0.62/0.54

[a]In THF at 1.0×10^{-5} M. [b]Determined for the Ln(III) emission peak under N_2. [c]In 10 wt % doped PMMA polymer films using an integration sphere.

To understand the origin of the absorption bands of the complexes shown in Figure 3, a TD-DFT computational study was carried out for all three free ligands and their sodium complexes Na_2L. The data obtained for the free ligands and their sodium complexes are comparable, and the details can be found in the SI. For the sodium complexes, the energies of vertical excitation to S_1 and S_2 are essentially identical, and the key contributions to these two transitions are shown in Figure 4. Both transitions are believed to be responsible for the absorption bands of the complexes at ~330 nm. The profiles of the calculated absorption spectra match very well with those shown in Figure 3. For all three ligands, the lowest unoccupied molecular orbital (LUMO) and LUMO + 1 levels are localized on the Na^+ ion. However, they make no contributions to the S_0 and S_1 transitions (see SI). As shown in Figure 4, the $S_0 \rightarrow S_1$ and $S_0 \rightarrow S_2$ excitations involve mainly the transitions of mesityl and duryl to the B atom for Na_2**L1** and Na_2**L2** with a very high oscillator strength, which could be described as mesityl → B and duryl → B CT transitions. In contrast, the $S_0 \rightarrow S_1$ and $S_0 \rightarrow S_2$ excitations for Na_2**L3** involve significant contributions from the phenyltriazolyl unit in addition to the mesityl with a high oscillator strength as well, which could be described as an admixture of mesityl → B-phenyltriazolyl CT and phenyltriazolyl → B-phenyltriazolyl $\pi \rightarrow \pi^*$ transitions. This is clearly caused by the greater π-conjugation in Na_2**L3** due to the less sterically demanding phenyl linker, compared to the duryl linker in Na_2**L1** and Na_2**L2**. The $S_0 \rightarrow T_1$ excitation involves a similar set of molecular orbitals as the $S_0 \rightarrow S_1$ state (see SI). Based on the TD-DFT data, the $BMes_2$-aryl unit is the key contributor to the first singlet and the triplet state with charge-transfer character. Although the TD-DFT-calculated excitation energies to S_1 and S_2 are similar for all three ligands, the excitation energy to the T_1 state is significantly lower for Na_2**L3** (431 nm/23200 cm^{-1}), compared to those of Na_2**L1** and Na_2**L2** (404 nm/24750 cm^{-1} and 406 nm/24630 cm^{-1}, respectively). Similar values were also obtained for the free ligands H_2**L1**, H_2**L2**, and H_2**L3** (see SI).

dx.doi.org/10.1021/ic501335e | Inorg. Chem. 2014, 53, 9751−9760

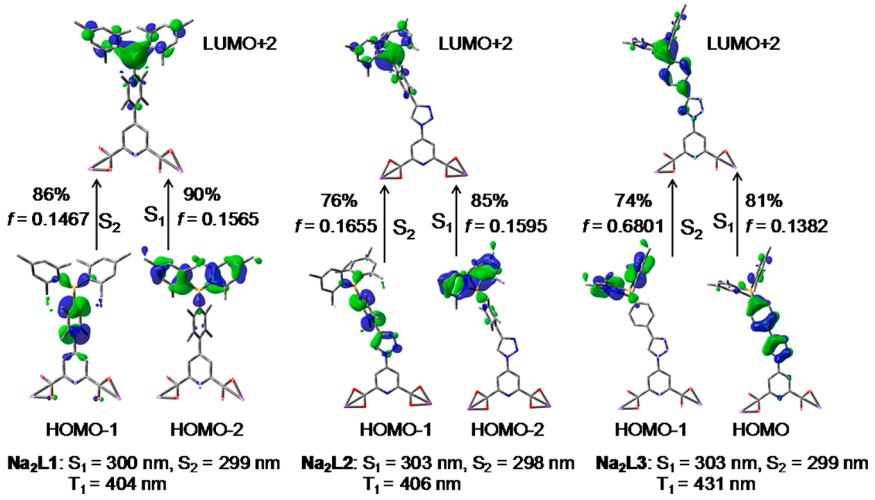

Figure 4. Key contributions to the $S_0 \rightarrow S_1$ and $S_0 \rightarrow S_2$ transitions of the ligands (as sodium complexes) obtained from TD-DFT data (MOs are plotted with an isocontour value of 0.04).

To determine the triplet energy levels experimentally, the phosphorescent spectra of $[NBu_4]_3[Gd\mathbf{L1}_3]$, $[NBu_4]_3[Gd\mathbf{L3}_3]$, and the free ligands $H_2\mathbf{L2}$ and $H_2\mathbf{L3}$ were recorded in frozen solution at 77 K using a time-resolved phosphorimeter (see SI).[23] For **L3**, the T_1 energies determined from the Gd(III) complex and the free ligand were the same, 435 nm/23000 cm^{-1}, validating that the T_1 energy could be obtained reliably by using either the Gd(III) complex or the free ligand. The experimental T_1 energies for **L1** and **L2** were indeed found to be similar, ~405 nm/24700 cm^{-1}. The experimentally determined T_1 energies of the ligands match very well with the TD-DFT-calculated T_1 energies for either the free ligands or the sodium complexes. Because the T_1 state of the activating ligand needs to be significantly higher [~3000 cm^{-1} for Tb(III)] than the emissive state of Tb(III) ($^5D_4$, 20500 cm^{-1}) and the emissive and accepting states of Eu(III) ($^5D_0$, 17250 cm^{-1}; $^5D_1$, 19000 cm^{-1}) to sensitize these Ln(III) ions,[10b,e,14d] **L1** and **L2** are expected to sensitize Tb(III) and Eu(III) emissions, whereas **L3** is predicted to be effective in sensitizing only Eu(III) emission because of its relatively low T_1 energy. Experimentally, however, **L2** and **L3** were found to be effective in sensitizing only Eu(III) emission, whereas **L1** is effective in sensitizing both Tb(III) and Eu(III) emissions.

As shown in Figure 5, all four Ln(III) complexes display bright Ln(III) emission in solution and the solid state. Both the ligand-centered blue fluorescent band and the Ln(III) emission bands were observed, and as a consequence, the Eu(III) compounds display a pink color, whereas the Tb(III) compound appears blue-green in solution. The emission spectra of the Ln(III) compounds are shown in Figure 6.

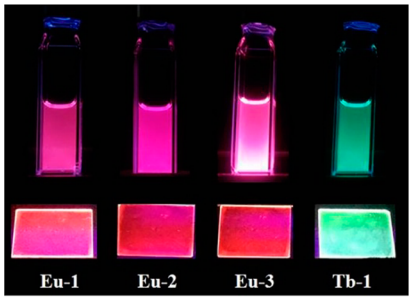

Figure 5. Photographs showing the emission colors of the Ln(III) complexes in THF and in PMMA films under UV light (365 nm).

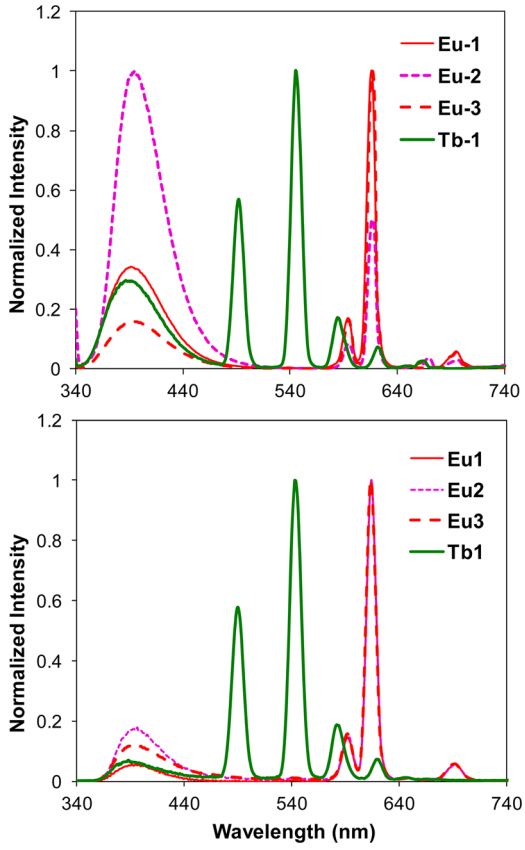

Figure 6. Luminescence spectra of the Ln(III) complexes (top) in solution (1.0×10^{-5} M in THF) and (bottom) in 10 wt % PMMA films with λ_{ex} = 330 nm.

The fluorescent peak of the complexes is attributed to ILCT of the ligands, as indicated by the TD-DFT data. The emission spectra show that **L1** is indeed effective in sensitizing both Tb(III) and Eu(III) emissions in solution and in the solid state. In the solid state, the ligand's fluorescence contributions to the emission spectra are the smallest for **Eu-1** and **Tb-1**, relative to

dx.doi.org/10.1021/ic501335e | Inorg. Chem. 2014, 53, 9751−9760

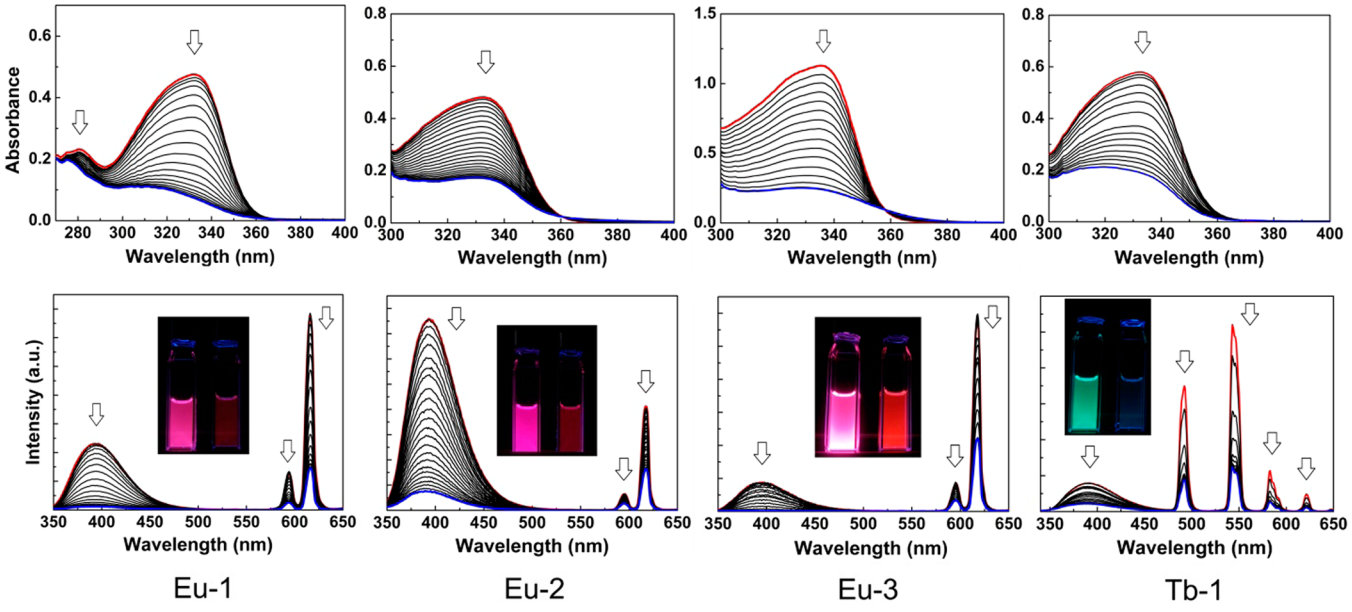

Figure 7. (Top) Absorption and (bottom) luminescence titration spectra of **Eu-1**, **Eu-2**, **Eu-3**, and **Tb-1** (1.0×10^{-5} M in THF) obtained using TBAF at 298 K (λ_{ex} = 330 nm) in THF. The inset photographs show the luminescence color changes of the solutions before and after TBAF addition.

those for **Eu-2** and **Eu-3**, indicating an efficient energy transfer from **L1** to the lanthanide center. The quantum efficiency of **Eu-1** in the solid state was measured to be 0.37 for the total emission and 0.30 for the Eu(III) emission (81% of the total emission). Similarly, the quantum efficiency for **Tb-1** was found to be 0.62 for total emission and 0.54 for Tb(III) emission (87% of the total emission), making it one of the brightest Tb(III) emitters known to date.[6,10e,24] The high T_1 energy of **L1** is clearly responsible for the effective sensitization of Tb(III) emission in **Tb-1**. In contrast, **Eu-2** shows weak Eu(III) emission with Φ_{Eu} = 0.07 and significant fluorescence from **L2**, especially in solution. This can be attributed to the fact that the first excited state of the ligand is localized mostly around the $BMes_2$(duryl) unit in **L2**, which is relatively far from the Eu(III) center in **Eu-2**, causing inefficient energy transfer to the Eu(III) ion. In comparison, the Eu(III) ion in **Eu-3** has a much higher emission quantum efficiency (Φ_{Eu} = 0.17) than that in **Eu-2**. This is in agreement with the TD-DFT data, which show that the ILCT and $\pi \rightarrow \pi^*$ transitions in **L3** involve the entire phenyltriazolyl unit because of the effective conjugation of the linker unit, thus shortening the energy-transfer distance and leading to more effective energy transfer to the Eu(III) unit in **Eu-3**. All of the Ln(III) complexes exhibit single-exponential decay in deoxygenated THF solutions, with decay lifetimes (τ) in the millisecond range, with the shortest for **Tb-1** (0.80 ms).

Impact of Fluoride Ions on Ln(III) Emission. Because the first excited state is localized on the $BMes_2Ar$ unit in all lanthanide compounds reported herein and because this unit is well-known for binding to small anions such as fluoride and cyanide, the lanthanide complexes could be used as receptors/sensors for these anions and for further probing of the role of the $BMes_2Ar$ unit in sensitizing Eu(III) or Tb(III) emission. We therefore examined the absorption and luminescence spectral changes of the Eu(III) and Tb(III) complexes upon titration with tetrabutylammonium fluoride (TBAF) in THF. The titration data for the Eu(III) and Tb(III) compounds as shown in Figure 7. The binding of the fluoride ion to the boron center was confirmed by the ^{19}F NMR titration spectrum of the **Eu-3** fluoride adduct (see SI), which displays a peak at −174 ppm, a value that is comparable to the ^{19}F chemical shift reported previously for a related $[BMes_2Ar(F)]^-$ species.[25]

Upon the addition of F^-, the ligand's fluorescence peak was either completely quenched (**Eu-3**) or partially quenched (**Eu-1**, **Eu-2**, and **Tb-1**), and the ligand's absorption band experienced a substantial decrease in intensity, which is in agreement with the assignment of the $S_0 \rightarrow S_1$ and $S_0 \rightarrow S_2$ transitions being ILCT involving the Mes/Ar group and the B atom and the binding of the F^- anion to the boron center. For all Eu(III) complexes, the Eu(III) emission peaks experienced partial quenching upon the addition of fluoride ions. For the **Tb-1** compound, the Tb(III) emission peaks were quenched, and the emission spectrum was dominated by **L1**'s fluorescence peak. As a consequence, the emission color of **Tb-1** changed from blue-green to deep blue, whereas that of the Eu(III) compounds changed from pink to red upon the addition of fluoride ions (Figures 7 and 8). Taking into consideration the absorbance changes at the excitation wavelength, the Ln(III) emission quantum efficiency of the fluoride adduct relative to the nonadduct was examined for each compound. For **Eu-1** and **Eu-2**, Φ_{Eu} did not change substantially after the addition of TBAF, whereas for **Eu-3**, it increased by 55%, as shown in Figure 9. For **Tb-1**, Φ_{Tb} dropped by 98%. Thus, the addition of TBAF turns on the emission of Eu(III) in **Eu-3**, whereas it turns off the Tb(III) emission in **Tb-1**. This phenomenon could be explained as follows:

Upon addition of fluoride ions, the boryl unit is switched from an electron-withdrawing group to an electron-donating group in the lanthanide complexes. As a result, the ILCT transition is likely switched from the Mes/Ar → B/Ar-triazolyl transition to the $BMes_2F(Ar)$ → triazolyl-dpa transition in the fluoride adducts of the Ln(III) complexes, as illustrated in Scheme 1, which causes the quenching of the ligand's fluorescence and the change of the ligand's triplet energy. For complexes with ligands **L1** and **L2**, which have orthogonal linkers, the addition of fluoride to the boron center is expected to decrease the T_1 energy because of the rise of the highest

dx.doi.org/10.1021/ic501335e | Inorg. Chem. 2014, 53, 9751−9760

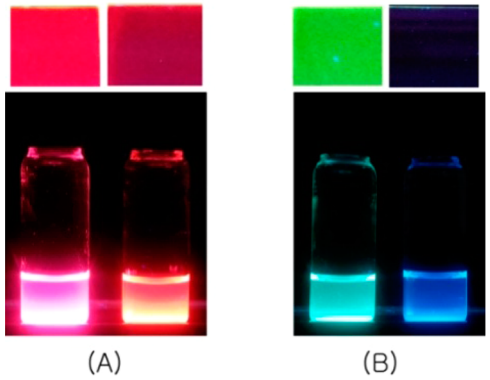

Figure 8. Photographs showing the luminescence color changes of (A) **Eu-3** and (B) **Tb-1** (top) in 10 wt % PMMA film and (bottom) in THF solution that contains PMMA [10 wt % of the solvent] (left) before and (right) after the addition of TBAF (excess) under 365-nm irradiation.

occupied molecular orbital (HOMO) level. For **Eu-3**, which has a conjugated linker unit in the ligand, the T_1 energy is expected to increase because of the destabilization of the LUMO level (π^*) due to the disruption of π-conjugation between the linker unit and the boron atom. Indeed, the T_1 energy of the fluoride adducts **Gd-1-F** and **Gd-2-F** determined from their phosphorescence spectra recorded at 77 K using a time-resolved phosphorimeter was found to shift to a lower energy (from 24600 to 24400 cm^{-1}), whereas that of **Gd-3-F** shifted to a higher energy (23300 to 23800 cm^{-1}) (see SI). The distinct geometry-dependent T_1 energy change was observed in $BMes_2Ar$-functionalized β-diketonato systems that we reported recently, in which compounds that have an orthogonal linker experience T_1 decreases whereas those with a conjugated linker experience T_1 increases upon fluoride addition.[6b] The T_1 energy decrease of **L1** is believed to be responsible for the quenching of the Tb(III) ion emission in **Tb-1-F**, whereas the T_1 energy increase of **L3** is likely responsible for the quantum efficiency enhancement of the Eu(III) emission in **Eu-3-F**. TD-DFT computational study for the boron-fluoride adducts of either the free ligands, H_2**L**, or the sodium complexes, Na_2**L**, were performed to further elucidate the impact of the fluoride ion. However, the results are not meaningful because of the multiple fluoride binding sites in these model compounds (e.g., the proton site and the Na^+ site).

The binding strengths of the Ln(III) complexes with fluoride ions are of the same order of magnitude as those of typical $BMes_2Ar$ compounds ($K \approx 10^4$–10^5 M^{-1}) reported previously,[17,18,25] as indicated by the binding constants of **Eu-2** [$K_1 = (3.2 \pm 1.0) \times 10^4$ M^{-1}, $K_2 = (8.1 \pm 0.8) \times 10^3$ M^{-1}, and $K_3 = (3.6 \pm 0.8) \times 10^3$ M^{-1}] estimated from the titration data (see SI). The evaluation of the binding strengths of the Ln(III) complexes with fluoride ions was complicated by the presence of varying amounts of water molecules associated with the different complexes, which were difficult to remove. Nonetheless, the emission spectral changes of all four complexes with TBAF are fully reversible upon the addition of water, which supports the structural integrity and high stability of these Ln(III) complexes. The emission spectra of the Ln(III) compounds have a similar response toward the addition of CN^- ions, as illustrated by the titration experiments of **Eu-1** and **Tb-1** with tetraethylammonium cyanide (TEACN) in THF (see SI). To demonstrate the selectivity of the Ln(III) compounds toward fluoride and cyanide ions, a titration experiment of **Eu-1** with TBACl was also performed. Not surprisingly, no appreciable absorption or emission spectral change was observed until a very large excess of TBACl (~70 equiv) had been added. The emission color of the Ln(III) complexes also changes upon the addition of fluoride ions in the presence of the PMMA polymer, as shown in Figure 8. The emission color changes of **Eu-3** and **Tb-1** in THF upon the addition of TBAF in the presence or absence of PMMA are similar. In 10 wt % PMMA films, the emission color change of **Tb-1** is quite sharp, from green to faint dark blue or nonemissive, whereas that of **Eu-3** is from red to dark red upon the addition of TBAF, illustrating the potential use of the new Ln(III) compounds in fluoride or cyanide sensing on a solid substrate.

CONCLUSIONS

The syntheses of three new dimesitylboron-functionalized dipicolinate ligands (H_2**L1**, H_2**L2**, and H_2**L3**) and their Eu(III) or Tb(III) complexes have been accomplished. The new ligands were found to be effective in the sensitization of Eu(III) or Tb(III) emission with high emission quantum efficiencies in the solid state. The $BMes_2Ar$ group was found to be intimately involved in ILCT transitions that play a key role in sensitizing the Ln(III) emission. The linker unit was found to greatly influence the T_1 energy of the ligand, leading to selective sensitization of Tb(III) or Eu(III) emission. The addition of anions such as fluoride ions was found to greatly influence the ILCT process, leading to distinct quenching or emission color switching of the Ln(III) compound, depending on the nature of

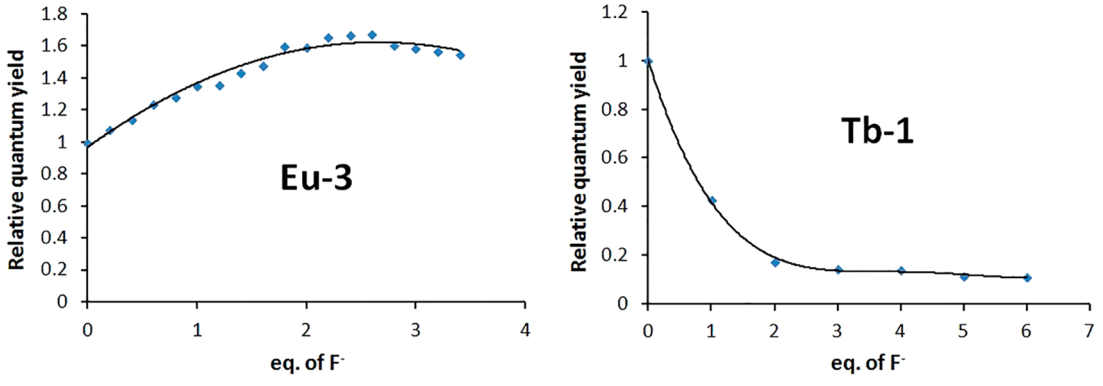

Figure 9. Relative quantum yield changes of **Eu-3** and **Tb-1** upon fluoride addition in THF.

dx.doi.org/10.1021/ic501335e | Inorg. Chem. 2014, 53, 9751–9760

the linker unit. Effective π-conjugation between the linker and the dpa unit in **L3** is responsible for its low T_1 energy, its selective sensitization of Eu(III) emission, and the fluoride-enhanced Eu(III) emission in **Eu-3**. In contrast, the orthogonal arrangement of the linker and the dpa unit in **L1** is responsible for its high T_1 energy, its selective sensitization, and the fluoride-induced quenching of Tb(III) emission in **Tb-1**.

■ ASSOCIATED CONTENT

Supporting Information

NMR spectra; phosphorescence spectra of **Gd-1**, **Gd-3**, and the free ligands at 77 K; excitation spectra; titration data; and TD-DFT calculation data for the free ligands and their sodium complexes. This material is available free of charge via the Internet at http://pubs.acs.org.

■ AUTHOR INFORMATION

Corresponding Author

*Tel.: +1-613-533-6941. Fax: +1-613-533-6669. E-mail: suning.wang@chem.queensu.ca.

Notes

The authors declare no competing financial interest.

■ ACKNOWLEDGMENTS

We thank the Natural Sciences and Engineering research Council of Canada for financial support. S.W. thanks the Canada Council for the Arts for a Killam Research Fellowship.

■ REFERENCES

(1) (a) Kido, J.; Okamoto, Y. *Chem. Rev.* **2002**, *102*, 2357. (b) Wang, J.; Wang, R.; Yang, J.; Zheng, Z.; Carducci, M. D.; Cayou, T.; Peyghambarian, N.; Jabbour, G. E. *J. Am. Chem. Soc.* **2001**, *123*, 6179–6180. (c) De Bettencourt-Dias, A. *Dalton Trans.* **2007**, 2229–2241. (d) Law, G. L.; Wong, K. L.; Tam, H. L.; Cheah, K. W.; Wong, W. T. *Inorg. Chem.* **2009**, *48*, 10492–10494. (e) Katkova, M. A.; Balashova, T. V.; Ilichev, V. A.; Konev, A. N.; Isachenkov, N. A.; Fukin, G. K.; Ketkov, S. Y.; Bochkarev, M. N. *Inorg. Chem.* **2010**, *49*, 5094–5100.

(2) Bünzli, J.-C. G. *Chem. Rev.* **2010**, *110*, 2729–2755.

(3) (a) Eliseeva, S. V.; Bünzli, J.-C. G. *Chem. Soc. Rev.* **2010**, *39*, 189–227. (b) TsuKube, H.; Shinoda, S. *Chem. Rev.* **2002**, *102*, 2389–2403. (c) Dos Santos, C. M. G.; Harte, A. J.; Quinn, S. J.; Gunnlaugsson, T. *Coord. Chem. Rev.* **2008**, *252*, 2512–2527. (d) Cheng, H.-B.; Zhang, H.-Y.; Liu, Y. *J. Am. Chem. Soc.* **2013**, *135*, 10190–10193. (e) Muller, G. *Dalton Trans.* **2009**, 9692–9707.

(4) (a) Mathis, G.; Bazin, H. In *Lanthanide Luminescence*; Hänninen, P., Härmä, H., Eds.; Springer: Berlin, 2010. (b) Moore, E. G.; Samuel, A. P. S.; Raymond, K. N. *Acc. Chem. Res.* **2009**, *42*, 542–552.

(5) (a) Park, D.; Senanayake, P. K.; Williams, J. A. G. *J. Chem. Soc., Perkin Trans.* **1998**, *2*, 2129–2140. (b) Parker, D. *Coord. Chem. Rev.* **2000**, *205*, 109–130. (c) Butler, S. J.; Parker, D. *Chem. Soc. Rev.* **2013**, *42*, 1652–1666. (d) Liu, T.; Nonat, A.; Beyler, M.; Regueiro-Figueroa, M.; Nono, K. N.; Jeannin, O.; Camerel, F.; Debaene, F.; Cianférani-Sanglier, S.; Tripier, R.; Platas-Iglesias, C.; Charbonnière, L. J. *Angew. Chem., Int. Ed.* **2014**, *53*, 7259–7263.

(6) (a) Varlan, M.; Blight, B. A.; Wang, S. *Chem. Commun.* **2012**, *48*, 12059–12061. (b) Smith, L. F.; Blight, B. A.; Park, H. J.; Wang, S. *Inorg. Chem.* **2014**, *53*, 8036–8044.

(7) Georges, J. *Analyst* **1993**, *118*, 1481–1486.

(8) Parker, D. *Chem. Soc. Rev.* **2004**, *33*, 156–165.

(9) (a) Yang, C.; Fu, L.-M.; Wang, Y.; Zhang, J.-P.; Wong, W.-T.; Ai, X.-C.; Qiao, Y.-F.; Zou, B.-S.; Gui, L.-L. *Angew. Chem., Int. Ed.* **2004**, *43*, 5010–5013. (b) Moudam, O.; Rowan, B. C.; Alamiry, M.; Richardson, P.; Richards, B. S.; Jones, A. C.; Robertson, N. *Chem. Commun.* **2009**, *45*, 6649–6651. (c) Walton, J. W.; Bourdolle, A.; Butler, S. J.; Soulie, M.; Delbianco, M.; McMahon, B. K.; Pal, R.; Puschmann, H.; Zwier, J. M.; Lamarque, L.; Maury, O.; Andraud, C.; Parker, D. *Chem. Commun.* **2013**, *49*, 1600–1602. (d) Miyata, K.; Nakagawa, T.; Kawakami, R.; Kita, Y.; Sugimoto, K.; Nakasima, T.; Harada, T.; Kawai, T.; Hasegawa, Y. *Chem.—Eur. J.* **2011**, *17*, 521–528. (e) Ma, Y.; Wang, Y. *Coord. Chem. Rev.* **2010**, *254*, 972–990.

(10) (a) Pandya, S.; Yu, J.; Parker, D. *Dalton Trans.* **2006**, 2757–2766. (b) Latva, M.; Takalo, H.; Mukkala, V.-M.; Matachescu, C.; Rodríguez-Ubis, J. C.; Kankare, J. *J. Lumin.* **1997**, *75*, 149–169. (c) EI Abidine Chamas, Z.; Guo, X.; Canet, J.-L.; Gautier, A.; Boyer, D.; Mahiou, R. *Dalton Trans.* **2010**, 7091–7097. (d) George, M. R.; Golden, C. A.; Grossel, M. C.; Curry, R. J. *Inorg. Chem.* **2006**, *45*, 1739–1744. (e) Aléo, A. D.; Pointillart, F.; Ouahab, L.; Andraud, C.; Maury, O. *Coord. Chem. Rev.* **2012**, *256*, 1604–1620.

(11) (a) Shavaleev, N. M.; Eliseeva, S. V.; Scopelliti, R.; Bünzli, J.-C. G. *Inorg. Chem.* **2010**, *49*, 3927–3936. (b) Andreiadis, E. S.; Demadrille, R.; Imbert, D.; Pecaut, J.; Mazzanti, M. *Chem.—Eur. J.* **2009**, *15*, 9458–9476. (c) De Bettencourt-Dias, A.; Viswanathan, S.; Rollett, A. *J. Am. Chem. Soc.* **2007**, *129*, 15436–15437. (d) Zebret, S.; Dupont, N.; Bernardinelli, G.; Hamacek, J. *Chem.—Eur. J.* **2009**, *15*, 3355–3358.

(12) (a) Sivakumar, S.; Reddy, M. L. P.; Cowley, A. H.; Vasudevan, K. V. *Dalton Trans.* **2010**, 776–786. (b) De Silva, C. R.; Li, J.; Zheng, Z.; Corrales, L. R. *J. Phys. Chem. A* **2008**, *112*, 4527–4530. (c) De Sá, G. F.; Malta, O. L.; Donega, C. D.; Simas, A. M.; Longo, R. L.; Santa-Cruz, P. A.; Da Silva, E. F. *Coord. Chem. Rev.* **2000**, *196*, 165–195.

(13) (a) Grenthe, I. *Acta Chem. Scand.* **1963**, *17*, 2487–2498. (b) Werts, M. H. V.; Jukes, R. T. F.; Verhoeven, J. W. *Phys. Chem. Chem. Phys.* **2002**, *4*, 1542–1548. (c) Aebischer, A.; Gumy, F.; Bünzli, J.-C. G. *Phys. Chem. Chem. Phys.* **2009**, *11*, 1346–1353.

(14) (a) Lamture, J. B.; Zhou, Z. H.; Kumar, A. S.; Wensel, T. G. *Inorg. Chem.* **1995**, *34*, 864–869. (b) D'Aléo, A.; Pompidor, G.; Elena, B.; Vicat, J.; Baldeck, P. L.; Toupet, L.; Kahn, R.; Andraud, C.; Maury, O. *ChemPhysChem* **2007**, *8*, 2125–2132. (c) D'Aléo, A.; Picot, A.; Baldeck, P. L.; Andraud, C.; Maury, O. *Inorg. Chem.* **2008**, *47*, 10269–10279. (d) D'Aléo, A.; Picot, A.; Beeby, A.; Williams, J. A. G.; Le Guennic, B.; Andraud, C.; Maury, O. *Inorg. Chem.* **2008**, *47*, 10258–10268. (e) Picot, A.; D'Aleo, A.; Baldeck, P. L.; Grichine, A.; Duperray, A.; Andraud, C.; Maury, O. *J. Am. Chem. Soc.* **2008**, *130*, 1532–1533. (f) Xiao, H.; Chen, M.; Mei, C.; Yin, H.; Zhang, X.; Cao, X. *Spectrochim. Acta A* **2011**, *84*, 238–244. (g) Nakamura, T.; Mizukami, S.; Tanaka, M.; Kikuchi, K. *Chem.—Asian J.* **2013**, *8*, 2685–2690. (h) Candelon, N.; Hâdade, N. D.; Matache, M.; Canet, J.-L.; Cisnetti, F.; Funeriu, D. P.; Nauton, L.; Gautier, A. *Chem. Commun.* **2013**, *49*, 9206–9208.

(15) Goodacre, R.; Shann, B.; Gilbert, R. J.; Timmins, E. M.; McGovern, A. C.; Alsberg, B. K.; Kell, D. B.; Logan, N. A. *Anal. Chem.* **2000**, *72*, 119–127.

(16) (a) Cable, M. L.; Kirby, J. P.; Sorasaenee, K.; Gray, H. B.; Ponce, A. *J. Am. Chem. Soc.* **2007**, *129*, 1474–1475. (b) Rieter, W. J.; Taylor, K. M.; Lin, W. *J. Am. Chem. Soc.* **2007**, *129*, 9852–9853. (c) Cable, M. L.; Kirby, J. P.; Levine, D. J.; Manary, M. J.; Gray, H. B.; Ponce, A. *J. Am. Chem. Soc.* **2009**, *131*, 9562–9570. (d) Yilmaz, M. D.; Hsu, S.-H.; Reinhoudt, D. N.; Velders, A. H.; Huskens, J. *Angew. Chem., Int. Ed.* **2010**, *49*, 5938–5941. (e) Clear, K. J.; Stroud, S.; Smith, B. D. *Analyst* **2013**, *138*, 7079–7082.

(17) (a) Wade, C. R.; Broomsgrove, A. E. J.; Aldridge, S.; Gabbaï, F. P. *Chem. Rev.* **2010**, *110*, 3958–3984. (b) Jäkle, F. *Chem. Rev.* **2010**, *110*, 3985–4022. (c) Entwistle, C. D.; Marder, T. B. *Chem. Mater.* **2004**, *16*, 4574–4585. (d) Entwistle, C. D.; Marder, T. B. *Angew. Chem., Int. Ed.* **2002**, *41*, 2927–2931. (e) Hudson, Z. M.; Wang, S. *Acc. Chem. Res.* **2009**, *42*, 1584–1596.

(18) (a) Yamaguchi, S.; Akiyama, S.; Tamao, K. *J. Am. Chem. Soc.* **2001**, *123*, 11372–11375. (b) You, Y. M.; Park, S. *Adv. Mater.* **2008**, *20*, 3820–3826. (c) Ito, A.; Kang, Y.; Saito, S.; Sakuda, E.; Kitamura, N. *Inorg. Chem.* **2012**, *51*, 7722–7732.

(19) Hudson, Z. M.; Sun, C.; Harris, K. J.; Lucier, B. E. G.; Schurko, R. W.; Wang, S. *Inorg. Chem.* **2011**, *50*, 3447–3457.

(20) Frisch, M. J.; Trucks, G. W.; Schlegel, H. B.; Scuseria, G. E.; Robb, M. A.; Cheeseman, J. R.; Scalmani, G.; Barone, V.; Mennucci, B.; Petersson, G. A.; Nakatsuji, H.; Caricato, M.; Li, X.; Hratchian, H.

P.; Izmaylov, A. F.; Bloino, J.; Zheng, G.; Sonnenberg, J. L.; Hada, M.; Ehara, M.; Toyota, K.; Fukuda, R.; Hasegawa, J.; Ishida, M.; Nakajima, T.; Honda, Y.; Kitao, O.; Nakai, H.; Vreven, T.; Montgomery, J. A., Jr.; Peralta, J. E.; Ogliaro, F.; Bearpark, M.; Heyd, J. J.; Brothers, E.; Kudin, K. N.; Staroverov, V. N.; Keith, T.; Kobayashi, R.; Normand, J.; Raghavachari, K.; Rendell, A.; Burant, J. C.; Iyengar, S. S.; Tomasi, J.; Cossi, M.; Rega, N.; Millam, J. M.; Klene, M.; Knox, J. E.; Cross, J. B.; Bakken, V.; Adamo, C.; Jaramillo, J.; Gomperts, R.; Stratmann, R. E.; Yazyev, O.; Austin, A. J.; Cammi, R.; Pomelli, C.; Ochterski, J. W.; Martin, R. L.; Morokuma, K.; Zakrzewski, V. G.; Voth, G. A.; Salvador, P.; Dannenberg, J. J.; Dapprich, S.; Daniels, A. D.; Farkas, Ö.; Foresman, J. B.; Ortiz, J. V.; Cioslowski, J.; Fox, D. J. *Gaussian 09*, revision B.01; Gaussian, Inc.: Wallingford, CT, 2010.

(21) (a) Tawada, Y.; Tsundeda, T.; Yanagisawa, S.; Yanai, T.; Hirao, K. *J. Chem. Phys.* **2004**, *120*, 8425−8433. (b) Guido, C.; Mennucci, B.; Jacquemin, D.; Adamo, C. *Phys. Chem. Chem. Phys.* **2010**, *12*, 8016−8023.

(22) Hay, P. J. *J. Phys. Chem. A* **2002**, *106*, 1634−1641.

(23) The triplet energy levels were determined by the lower-wavelength emission edges of the phosphorescence spectra at 77 K.

(24) (a) Biju, S.; Reddy, M. L. P.; Cowley, A. H.; Vasuderan, K. V. *J. Mater. Chem.* **2009**, *19*, 5179−5187. (b) Sivakumar, S.; Reddy, M. L. P. *J. Mater. Chem.* **2012**, *22*, 10852−10859. (c) Andreiadis, E. S.; Gauthier, N.; Imbert, D.; Demadrille, R.; Pécaut, J.; Mazzanti, M. *Inorg. Chem.* **2013**, *52*, 14382−14390.

(25) (a) Liu, X. Y.; Bai, D. R.; Wang, S. *Angew. Chem., Int. Ed.* **2006**, *45*, 5475. (b) Hudson, Z. M.; Liu, X.; Wang, S. *Org. Lett.* **2011**, *13*, 300−303. (c) Solé, S.; Gabbaï, F. P. *Chem. Commun.* **2004**, 1284−1285.